

# Biomimetic Oxygen Activation by MoS<sub>2</sub>/Ta<sub>3</sub>N<sub>5</sub> Nanocomposites for Selective Aerobic Oxidation\*\*

Qingsheng Gao,\* Cristina Giordano, and Markus Antonietti

The selective oxidation of petroleum-based feedstocks to useful functionalized chemicals is an important family of chemical transformations.<sup>[1]</sup> Of these transformations, the selective oxidation of alcohols, alkenes, amines, and sulfides are among the most challenging reactions in green chemistry.<sup>[2]</sup> There is significant interest in the design of new, cost-effective, and environmentally friendly heterogeneous catalysts that use molecular oxygen (O<sub>2</sub>) under mild conditions, to avoid the use of a large excess of toxic and expensive stoichiometric metal oxidants.<sup>[1,3]</sup> Although a number of catalysts based on novel metals and transition-metal oxides have been introduced,<sup>[4]</sup> the precise design of catalysts with well-defined behaviors that depend on surface properties and electron features is still desired. Such catalysts are significant not only for use with multifunctional substrates, but also for insightful studies of catalytic mechanisms. These challenges are expected to be met through facet engineering and component control at the catalyst surface and in the active sites on the level of nanochemistry.<sup>[5]</sup>

Crystal-facet engineering has been successfully introduced to exploit novel metal nanocatalysts with high-surface-energy planes. This approach has led to high activity and selectivity in oxidation catalysis.<sup>[5b,e,6]</sup> However, it is difficult to control facet growth in metal-oxide catalysts with low-symmetry crystal structures owing to the complexity of their structures.<sup>[7]</sup> On the other hand, the ability to effectively vary the surface properties and electronic features of metal oxides by doping with other elements of different electronegativity, such as N, P, and S, enables new strategies for catalyst design.<sup>[8]</sup> For example, the introduction of N into metal oxides can increase the energy of the HOMO orbital and narrow the band gap to thus enhance the catalytic activity,<sup>[9]</sup> although controlled nitridation is difficult by current synthetic strategies. Recently, we proposed Ca<sup>2+</sup>- and SiO<sub>2</sub>-assisted urea methods for the controlled nitridation of transition metals.

Remarkably, we discovered tunable oxidation ability associated with tailored nitridation,<sup>[10]</sup> namely, improved activity and tunable selectivity for alkene epoxidation on TaON and Ta<sub>3</sub>N<sub>5</sub> nanoparticles (NPs) with H<sub>2</sub>O<sub>2</sub>. This discovery opens up opportunities to develop superior tantalum-based catalysts with well-defined properties, especially for reactions involving cheap O<sub>2</sub> as the oxidant. Access to such catalysts is needed to enable the important factors for catalytic turnover and selectivity to be uncovered. However, the absence of O<sub>2</sub> activation in such (oxy)nitrides synthesized so far seriously limits further exploration.

Biomimetic studies point to a new way to develop catalysts by learning from nature. In nature, the active center of nitrogenase enzymes contains metal atoms usually bound to sulfur, such as active Mo–S and Fe–S clusters.<sup>[11]</sup> In nitrogen fixation, Mo–S and Fe–S sites activate inert N<sub>2</sub> to react with H<sup>+</sup>, with the generation of NH<sub>3</sub> and H<sub>2</sub>.<sup>[11,12]</sup> This process inspired the use of MoS<sub>x</sub> for electro- and photo-electrocatalytic H<sub>2</sub> evolution based on electron transfer from MoS<sub>2</sub> to H<sup>+</sup>.<sup>[12,13]</sup> The close energy potentials of  $E^0(\text{H}^+/\text{H}_2) = 0 \text{ V}$  and  $E^0(\text{O}_2/\text{O}_2^-) = -0.16 \text{ V}$  versus the normal hydrogen electrode<sup>[14]</sup> suggest that MoS<sub>x</sub> could be used as a biomimetic O<sub>2</sub>-activation reagent to exploit bifunctional tantalum-based nanocatalysts for aerobic oxidation reactions.

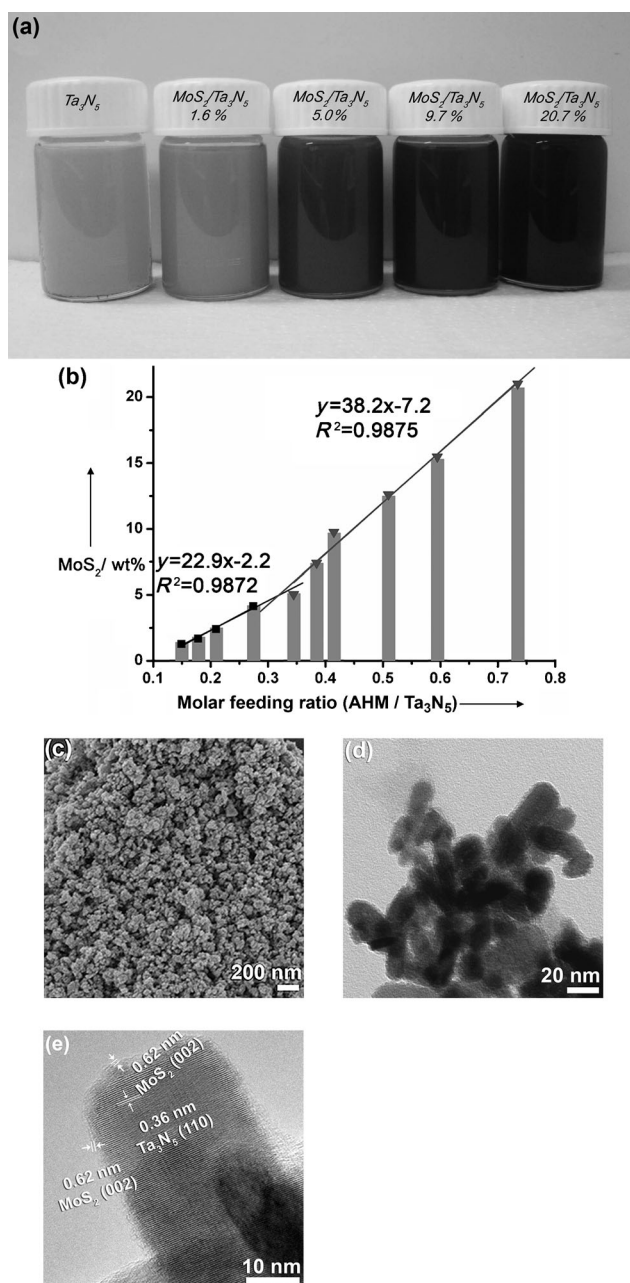
Herein, we describe the development of a new MoS<sub>2</sub>/Ta<sub>3</sub>N<sub>5</sub> catalyst in which Ta<sub>3</sub>N<sub>5</sub> NPs are integrated with ultrathin MoS<sub>2</sub> layers on the nanoscale by a hydrothermal method. The MoS<sub>2</sub> nanolayers act as a biomimetic O<sub>2</sub>-activation reagent in the MoS<sub>2</sub>/Ta<sub>3</sub>N<sub>5</sub> NPs, which showed high activity and selectivity in the aerobic oxidation of alcohols as a result of the synergistic effect between MoS<sub>2</sub> and Ta<sub>3</sub>N<sub>5</sub>. The MoS<sub>2</sub>/Ta<sub>3</sub>N<sub>5</sub> NPs were also active in the aerobic oxidation of alkenes, amines, and sulfides. The different activities observed for these different substrates imply the potential use of this catalyst with multifunctional substrates. For example, high selectivity for hydroxy-group oxidation (>90%) was observed in the oxidation of unsaturated alcohols.

Well-defined Ta<sub>3</sub>N<sub>5</sub> NPs of approximately 20 nm in diameter were prepared by our previously reported SiO<sub>2</sub>-assisted urea method (see Figure S1 in the Supporting Information).<sup>[10a]</sup> Hydrothermal treatment of the Ta<sub>3</sub>N<sub>5</sub> NPs with varying amounts of ammonium heptamolybdate (AHM) and thiourea at 180 °C for 20 h (see the Supporting Information) gave a series of MoS<sub>2</sub>/Ta<sub>3</sub>N<sub>5</sub> nanocomposites that varied in their MoS<sub>2</sub> content. The color of the composites changed from red to black as the MoS<sub>2</sub> content increased (Figure 1a; see also Figure S2 in the Supporting Information). Inductively coupled plasma analysis and CHNS elemental analysis were used to determine the Mo and S content, respectively. The

[\*] Dr. Q. S. Gao, Dr. C. Giordano, Prof. Dr. M. Antonietti  
Department of Colloid Chemistry, Max Planck Institute of Colloids and Interfaces, Research Campus Golm  
14424 Potsdam (Germany)  
E-mail: qingsheng.gao@mpikg.mpg.de  
Dr. Q. S. Gao  
Department of Chemistry, Jinan University  
510632 Guangzhou (P.R. China)  
E-mail: tqsgao@jnu.edu.cn

[\*\*] We acknowledge financial support from the BMBF (Project No. 035F0353A-E), the Max Planck Society, and the NSFC (21203075). Q.S.G. thanks Dr. X. Liu and K. Otte of MPIKG for SEM, and Prof. C. Y. Liu and M. Meng of Jinan University for fruitful discussions.

Supporting information for this article is available on the WWW under <http://dx.doi.org/10.1002/anie.201206542>.



**Figure 1.** a) Photographs of as-obtained  $\text{MoS}_2/\text{Ta}_3\text{N}_5$  NPs dispersed in EtOH. b)  $\text{MoS}_2$  loading content of the  $\text{MoS}_2/\text{Ta}_3\text{N}_5$  NPs with respect to the AHM/ $\text{Ta}_3\text{N}_5$  feeding ratio. c) SEM, d) TEM, and e) high-resolution TEM images of  $\text{MoS}_2/\text{Ta}_3\text{N}_5$ -5.0 NPs with 5.0 wt%  $\text{MoS}_2$ .

obtained Mo/S molar ratio is close to the theoretical value (0.5), which confirms the  $\text{MoS}_2$  stoichiometry. The correlation between the  $\text{MoS}_2$  loading and the AHM/ $\text{Ta}_3\text{N}_5$  feeding ratio (Figure 1b) suggests the potential of our method for the design of various  $\text{MoS}_2/\text{Ta}_3\text{N}_5$  composites of defined composition. The small slope difference in the ranges of low and high feeding ratios is due to the surface basicity of  $\text{Ta}_3\text{N}_5$ ,<sup>[10a]</sup> since the basic surface will partly dissolve  $\text{MoS}_2$ . Herein, the series of  $\text{MoS}_2/\text{Ta}_3\text{N}_5$  nanoparticles with different compositions are denoted as  $\text{MoS}_2/\text{Ta}_3\text{N}_5$ - $n$ , in which  $n$  refers to the  $\text{MoS}_2$  content ( $n\%$ ).

The preservation of the  $\text{Ta}_3\text{N}_5$  phase in the as-obtained  $\text{MoS}_2/\text{Ta}_3\text{N}_5$  nanocomposites is well confirmed by their X-ray diffraction patterns (see Figure S3 in the Supporting Information). Scanning electron microscopy (SEM) also confirmed the retention of the shape and size of the NPs in the products. Thus, both SEM and TEM images of  $\text{MoS}_2/\text{Ta}_3\text{N}_5$ -5.0 displayed well-defined NPs with a size of about 20 nm (Figure 1c,d). Furthermore, the  $\text{Ta}_3\text{N}_5$  NPs coated with ultra-thin  $\text{MoS}_2$  layers were revealed well by TEM (Figure 1e), in which the characteristic lattice fringes of  $\text{MoS}_2$  and  $\text{Ta}_3\text{N}_5$  were detected. The combination of these materials on the nanoscale was expected to have a great effect on their catalytic behavior.

The aerobic oxidation of benzyl alcohol (BA) was carried out as the test reaction for our  $\text{MoS}_2/\text{Ta}_3\text{N}_5$  nanocatalysts (Table 1). Bare  $\text{Ta}_3\text{N}_5$  NPs did not promote the conversion of

**Table 1:** Study of the reaction conditions.<sup>[a]</sup>

$\text{C}_6\text{H}_5\text{CH}_2\text{OH} + 1/2 \text{O}_2 \longrightarrow \text{C}_6\text{H}_5\text{CHO}$				
Entry	Catalyst	Atm.	Conv. [%]	Sel. [%]
1	$\text{Ta}_3\text{N}_5$	$\text{O}_2$	—	—
2 <sup>[b]</sup>	$\text{Ta}_3\text{N}_5$	Air	44	99
3	$\text{MoS}_2$	$\text{O}_2$	17	90
4 <sup>[c]</sup>	$\text{MoS}_2 + \text{Ta}_3\text{N}_5$	$\text{O}_2$	—	—
5	$\text{MoS}_2/\text{Ta}_3\text{N}_5$ -1.3	$\text{O}_2$	9	99
6	$\text{MoS}_2/\text{Ta}_3\text{N}_5$ -1.6	$\text{O}_2$	32	99
7	$\text{MoS}_2/\text{Ta}_3\text{N}_5$ -4.2	$\text{O}_2$	90	99
8	$\text{MoS}_2/\text{Ta}_3\text{N}_5$ -5.0	$\text{O}_2$	98	99
9	$\text{MoS}_2/\text{Ta}_3\text{N}_5$ -7.4	$\text{O}_2$	93	98
10	$\text{MoS}_2/\text{Ta}_3\text{N}_5$ -9.7	$\text{O}_2$	64	99
11	$\text{MoS}_2/\text{Ta}_3\text{N}_5$ -13.5	$\text{O}_2$	62	99
12	$\text{MoS}_2/\text{Ta}_3\text{N}_5$ -20.7	$\text{O}_2$	56	99
13 <sup>[d]</sup>	$\text{MoS}_2/\text{Ta}_3\text{N}_5$ -5.0	Air	10	99
14	$\text{MoS}_2/\text{Ta}_3\text{N}_5$ -5.0	$\text{N}_2$	—	—
15 <sup>[e]</sup>	$\text{Ta}_3\text{N}_5$	$\text{O}_2$	—	—

[a] Reaction conditions: benzyl alcohol (2 mmol), catalyst (40 mg),  $N,N$ -dimethylacetamide (4 mL),  $\text{O}_2$  balloon (1 atm), 120 °C, 3 h. [b]  $\text{H}_2\text{O}_2$  was used as the oxidant. [c] A physical mixture of  $\text{MoS}_2$  and  $\text{Ta}_3\text{N}_5$  was used ( $\text{MoS}_2$ : 5.0 wt %). [d] Reaction time: 9 h. [e]  $\text{Ta}_3\text{N}_5$  was treated with thiourea in a hydrothermal process, 180 °C, 20 h.

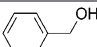
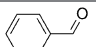
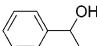
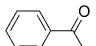
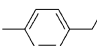
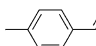
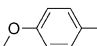
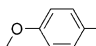
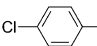
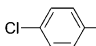
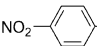
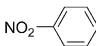
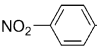
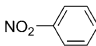
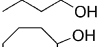
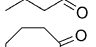
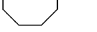

BA, although they were active when  $\text{H}_2\text{O}_2$  was used as the oxidant (Table 1, entries 1 and 2); thus,  $\text{O}_2$  activation does not appear to occur on  $\text{Ta}_3\text{N}_5$ . Bare  $\text{MoS}_2$  only exhibited low activity for the aerobic oxidation of BA, and no BA conversion was observed with a physical mixture of  $\text{MoS}_2$  and  $\text{Ta}_3\text{N}_5$  (Table 1, entries 3 and 4). Surprisingly, the  $\text{MoS}_2/\text{Ta}_3\text{N}_5$  nanocomposites displayed significantly improved activity with 99% selectivity for the formation of benzaldehyde under the same reaction conditions (Table 1, entries 5–12). The catalytic activity can be optimized by adjusting the  $\text{MoS}_2$  content, whereby complete BA conversion was observed for nanocomposites with an  $\text{MoS}_2$  content ranging from 5.0 to 6.0% (see Figure S4 in the Supporting Information).

We used the  $\text{MoS}_2/\text{Ta}_3\text{N}_5$ -5.0 NPs to further explore the catalytic behavior of our catalysts. The dramatic decrease in catalytic activity when the reaction was carried out in air and the complete loss of activity in a  $\text{N}_2$  atmosphere (Table 1,

entries 13 and 14) indicated that the oxidation of BA relies on catalytic processes involving  $O_2$  and the  $MoS_2/Ta_3N_5$  NPs. A possible effect on the catalyst of hydrothermal treatment with thiourea could be disregarded following the observation that no BA conversion occurred on  $Ta_3N_5$  NPs that had been treated with thiourea (Table 1, entry 15). Thus, we could confirm the biomimetic activation of  $O_2$  by the  $MoS_2$  nanolayers. Although a slight deactivation was observed after three cycles, probably as a result of the partial dissolution of  $MoS_2$  by peroxide species formed in situ, the activity of  $MoS_2/Ta_3N_5$  was recovered well by repeating the hydrothermal process (see Figure S5 in the Supporting Information).

In a further set of experiments, we examined the efficacy of the transformation of alcohols into aldehydes under the optimized reaction conditions (Table 2).  $MoS_2/Ta_3N_5$ -5.0

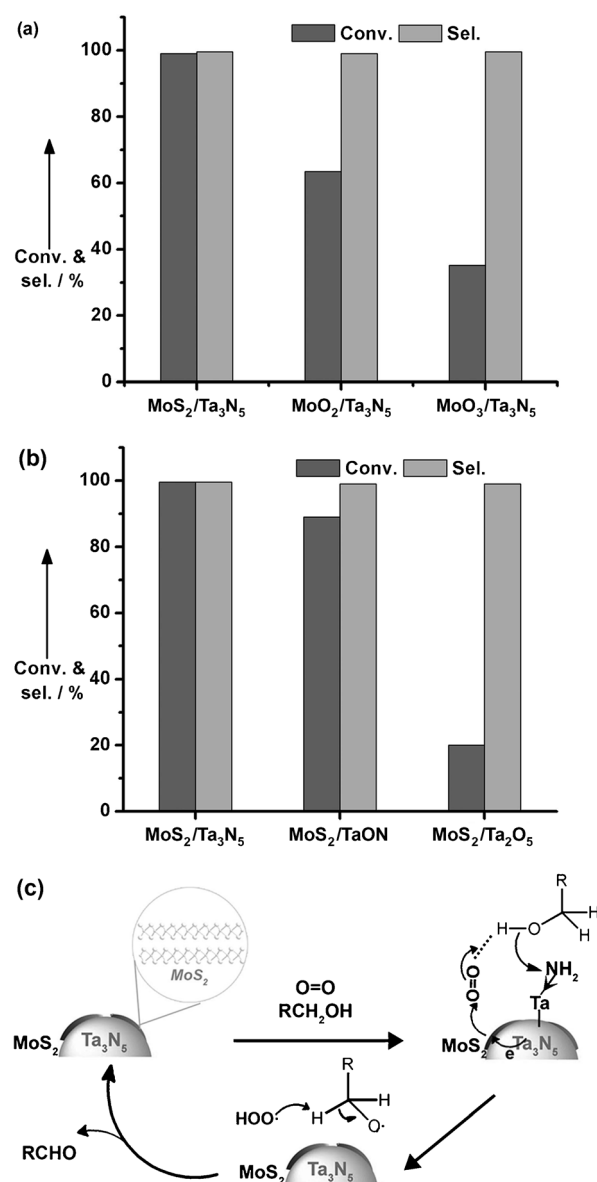
**Table 2:** Selective oxidation of alcohols.<sup>[a]</sup>

Entry	Substrate	Selectivity [%]	Conv. [%]	T [h]	
1			99	85	1.5
2			99	88	1.5
3			99	99	1.5
4			99	99	1.5
5			96	74	1.5
6			99	36	1.5
7			99	86	3.0
8			99	80	4.0
9			99	80	2.0

[a] Reaction conditions: alcohol (1 mmol),  $MoS_2/Ta_3N_5$ -5.0 (40 mg), *N,N*-dimethylacetamide (4 mL),  $O_2$  balloon (1 atm), 120 °C.

showed high versatility. The catalyst was highly active and extremely selective for the aerobic oxidation of all substrates tested. Substituted benzyl alcohols containing electron-donating groups (such as  $-CH_3$  or  $-OCH_3$ ; Table 2, entries 3 and 4) were more readily oxidized than those containing electron-withdrawing groups (such as  $-Cl$  and  $-NO_2$ ; Table 2, entries 5–7). In the latter case, the reaction is even slower than that of unsubstituted benzyl alcohol. Our  $MoS_2/Ta_3N_5$ -5.0 nanocatalyst also exhibited high activity and selectivity for the aerobic oxidation of aliphatic and alicyclic alcohols (Table 2, entries 8 and 9).

Under the same conditions,  $MoS_2/Ta_3N_5$ -5.0 did not catalyze BA oxidation in the presence of butylated hydroxytoluene, a terminating reagent that suppresses autoxidation (a free-radical chain process). This result strongly suggests that the reaction in our catalytic system involves the formation of the superoxide radical anion ( $\cdot O_2^-$ ).<sup>[15]</sup> Furthermore, we found that the activity of our catalyst depends on the Mo additive used. For example, with the same loading content



**Figure 2.** a) Effect of the Mo species and b) effect of the nitridation level on the catalytic performance (conversion, selectivity) of tantalum-based NPs in the aerobic oxidation of BA (the amount of the Mo additive in the nanocomposites was fixed at 5.0 wt %). Reaction conditions: BA (2 mmol), catalyst (40 mg), *N,N*-dimethylacetamide (4 mL),  $O_2$  balloon (1 atm), 120 °C, 3 h. c) Schematic illustration of the catalytic mechanism of the  $MoS_2/Ta_3N_5$  nanocatalyst.

of 5.0%,  $MoS_2/Ta_3N_5$  displayed the highest activity of the three  $Ta_3N_5$  catalysts formed by modification with  $MoS_2$ ,  $MoO_2$ , and  $MoO_3$  (Figure 2a), which implies that  $MoS_2$  has the best  $O_2$ -activation ability. On the other hand, the nitridation level of the tantalum-based NPs also affected their catalytic activity according to the order  $Ta_3N_5 > TaON > Ta_2O_5$  (Figure 2b). We suggest that the enhanced oxidation ability of tantalum-based nanocatalysts results from the tailored introduction of N atoms, the electronegativity of which is lower than that of O atoms.<sup>[10a]</sup>

The combination of  $MoS_2$  and  $Ta_3N_5$  on the nanoscale is the key to the superior catalytic behavior of  $MoS_2/Ta_3N_5$ ;

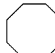
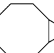
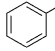
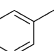
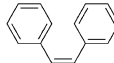
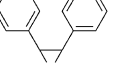
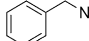
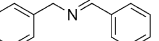
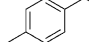
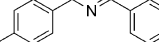
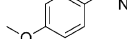
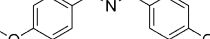
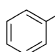
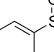
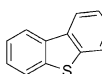
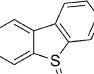
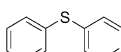
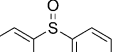
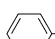
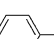
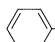
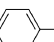

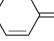


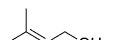
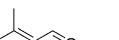
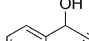
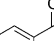


therefore, the interaction of these components at the nano-interface should be taken in account in the proposed catalytic mechanism (Figure 2c). During O<sub>2</sub> activation, the donation of an electron from MoS<sub>2</sub> to molecular O<sub>2</sub> is promoted by electron transfer from tantalum-based NPs (see Figure S6 in the Supporting Information). This process is similar to that observed at Schottky junctions.<sup>[16]</sup> The increased electron density around Ta and increased HOMO energy upon the introduction of nitrogen atoms facilitates electron transfer,<sup>[9,10]</sup> and the activity of the catalyst depends on the nitridation level. Thus, the HOMO orbitals that lose electrons are considered the oxidation sites on Ta<sub>3</sub>N<sub>5</sub> for alcohol oxidation with activated <sup>•</sup>O<sub>2</sub>.<sup>[14]</sup> In this mechanism, the combination of MoS<sub>2</sub> and Ta<sub>3</sub>N<sub>5</sub> on the nanoscale is indispensable for the reaction, as confirmed by the lack of BA conversion detected in the presence of a physical mixture of these catalyst components (Table 1, entry 4). Thus, MoS<sub>2</sub>/Ta<sub>3</sub>N<sub>5</sub> nanocatalysts integrate the features of both MoS<sub>2</sub> and tantalum-based NPs; O<sub>2</sub> activation on MoS<sub>2</sub> and alcohol oxidation by the tantalum sites are synergistically enhanced through interaction on the nanoscale.

Our MoS<sub>2</sub>/Ta<sub>3</sub>N<sub>5</sub> NPs could be considered in a sense as a universal catalyst for the aerobic oxidation of various functional groups, including alcohols, alkenes, amines, and sulfides. The MoS<sub>2</sub>/Ta<sub>3</sub>N<sub>5</sub>-5.0 nanocatalysts were found to be active for the epoxidation of cyclooctene, styrene, and *cis*-stilbene (according to structure shown) with O<sub>2</sub> as the oxidant (Table 3, entries 1–3). For the example of cyclooctene epoxidation, the performance of the catalyst is associated with the MoS<sub>2</sub> loading, the Mo species, and the nitridation level of the tantalum-based NPs (see Figure S7 in the Supporting Information). These observations are consistent with the results for BA oxidation and further support the proposed catalytic mechanism. In the case of amine and sulfide substrates, MoS<sub>2</sub>/Ta<sub>3</sub>N<sub>5</sub> shows lower activity than for BA oxidation under the same conditions (Table 3, entries 4–9). As commonly accepted, amines and sulfides can be oxidized more readily than alcohols; however, they unfortunately have a poisoning effect on many catalysts.<sup>[17]</sup> In the presence of thioanisole or phenethylamine, the conversion of BA was dramatically decreased (Table 3, entries 10 and 11). This observation confirms the ready poisoning of MoS<sub>2</sub>/Ta<sub>3</sub>N<sub>5</sub> by -SH and -NH<sub>2</sub> groups, probably as a result of their strong combination with Mo exposed on MoS<sub>2</sub> edges.<sup>[18]</sup>

The better activity of MoS<sub>2</sub>/Ta<sub>3</sub>N<sub>5</sub> NPs for alcohol oxidation relative to that for alkene oxidation suggests the potential of this catalyst for the selective oxidation of unsaturated alcohols. Remarkably high selectivity (>90%) was observed for hydroxy-group oxidation on MoS<sub>2</sub>/Ta<sub>3</sub>N<sub>5</sub>-5.0, as well as high activity (Table 3, entries 12–16). This well-defined catalytic behavior of MoS<sub>2</sub>/Ta<sub>3</sub>N<sub>5</sub> NPs will promote their use for the oxidation of multifunctional substrates. They will also be useful in catalyst design and mechanistic studies.

In summary, MoS<sub>2</sub> was used as a biomimetic O<sub>2</sub>-activation reagent to construct a new catalyst with high activity and selectivity in the aerobic oxidation of alcohols. The superior catalytic behavior results from the combination of Ta<sub>3</sub>N<sub>5</sub> and MoS<sub>2</sub> on the nanoscale and the synergistic enhancement of the effects of these two components. The resulting catalyst can

**Table 3:** Selective oxidation of alkenes, amines, sulfides, and unsaturated alcohols.<sup>[a]</sup>

Entry	Substrates	Selectivity [%]	Conv. [%]	T [h]	
1			94	49	6.0
2			48	75	6.0
3			93	50	6.0
4			99	41	3.0
5			99	52	3.0
6			99	50	3.0
7			99	50	3.0
8			99	43	3.0
9			86	33	3.0
10 <sup>[b]</sup>			99	10	3.0
11 <sup>[c]</sup>			99	11	3.0
12			99	78	3.0
13			93	99	1.5
14			99	99	3.0
15			99	66	3.0
16			98	99	3.0

[a] Reaction conditions: substrate (1 mmol), MoS<sub>2</sub>/Ta<sub>3</sub>N<sub>5</sub>-5.0 (40 mg), *N,N*-dimethylacetamide (4 mL), O<sub>2</sub> balloon (1 atm), 120°C. [b] The reaction was carried out in the presence of thioanisole (1 mmol). [c] The reaction was carried out in the presence of phenethylamine (1 mmol).

be considered universally active for the oxidation of alkenes, amines, and sulfides. The different performance observed for the oxidation of various functional groups makes MoS<sub>2</sub>/Ta<sub>3</sub>N<sub>5</sub> a highly selective catalyst for use with multifunctional substrates, such as unsaturated alcohols. Owing to the facile synthesis and tunable properties of the MoS<sub>2</sub>/Ta<sub>3</sub>N<sub>5</sub> NPs, we believe that our efforts will pave the way for the design of a range of efficient metal-based nanocatalysts.

Received: August 14, 2012

Published online: October 12, 2012

**Keywords:** molybdenum sulfide · nanocomposites · O–O activation · selective oxidation · tantalum nitrides



- [1] T. Punniyamurthy, S. Velusamy, J. Iqbal, *Chem. Rev.* **2005**, *105*, 2329.
- [2] a) T. Mallat, A. Baiker, *Chem. Rev.* **2004**, *104*, 3037; b) M. D. Hughes, Y. J. Xu, P. Jenkins, P. McMorn, P. Landon, D. I. Enache, A. F. Carley, G. A. Attard, G. J. Hutchings, F. King, E. H. Stitt, P. Johnston, K. Griffin, C. J. Kiely, *Nature* **2005**, *437*, 1132; c) G. J. ten Brink, I. Arends, R. A. Sheldon, *Science* **2000**, *287*, 1636; d) K. Yamaguchi, N. Mizuno, *Angew. Chem.* **2003**, *115*, 1518; *Angew. Chem. Int. Ed.* **2003**, *42*, 1480; e) L. Chen, Y. Yang, D. L. Jiang, *J. Am. Chem. Soc.* **2010**, *132*, 9138.
- [3] R. A. Sheldon, I. Arends, G. J. Ten Brink, A. Dijkman, *Acc. Chem. Res.* **2002**, *35*, 774.
- [4] a) A. Corma, H. Garcia, *Chem. Soc. Rev.* **2008**, *37*, 2096; b) G. J. Hutchings, *Chem. Commun.* **2008**, 1148; c) N. Yan, C. X. Xiao, Y. Kou, *Coord. Chem. Rev.* **2010**, *254*, 1179.
- [5] a) G. A. Somorjai, H. Frei, J. Y. Park, *J. Am. Chem. Soc.* **2009**, *131*, 16589; b) K. B. Zhou, Y. D. Li, *Angew. Chem.* **2012**, *124*, 622; *Angew. Chem. Int. Ed.* **2012**, *51*, 602; c) G. Pacchioni, *J. Chem. Phys.* **2008**, *128*, 182505; d) Z. P. Hu, B. Li, X. Y. Sun, H. Metiu, *J. Phys. Chem. C* **2011**, *115*, 3065; e) Z. Y. Zhou, N. Tian, J. T. Li, I. Broadwell, S. G. Sun, *Chem. Soc. Rev.* **2011**, *40*, 4167.
- [6] N. Tian, Z. Y. Zhou, S. G. Sun, Y. Ding, Z. L. Wang, *Science* **2007**, *316*, 732.
- [7] C. N. R. Rao, H. Matte, R. Voggu, A. Govindaraj, *Dalton Trans.* **2012**, *41*, 5089.
- [8] a) R. Asahi, T. Morikawa, T. Ohwaki, K. Aoki, Y. Taga, *Science* **2001**, *293*, 269; b) Z. W. Liu, F. Peng, H. J. Wang, H. Yu, W. X. Zheng, J. A. Yang, *Angew. Chem.* **2011**, *123*, 3315; *Angew. Chem. Int. Ed.* **2011**, *50*, 3257; c) Y. D. Xia, R. Mokaya, *J. Phys. Chem. C* **2008**, *112*, 1455.
- [9] K. Maeda, K. Domen, *J. Phys. Chem. C* **2007**, *111*, 7851.
- [10] a) Q. S. Gao, S. N. Wang, Y. C. Ma, Y. Tang, C. Giordano, M. Antonietti, *Angew. Chem.* **2012**, *124*, 985; *Angew. Chem. Int. Ed.* **2012**, *51*, 961; b) Q. S. Gao, C. Giordano, M. Antonietti, *Small* **2011**, *7*, 3334.
- [11] G. Schwarz, R. R. Mendel, M. W. Ribbe, *Nature* **2009**, *460*, 839.
- [12] A. B. Laursen, S. Kegnaes, S. Dahl, I. Chorkendorff, *Energy Environ. Sci.* **2012**, *5*, 5577.
- [13] H. Vrubel, D. Merki, X. L. Hu, *Energy Environ. Sci.* **2012**, *5*, 6136.
- [14] F. Z. Su, S. C. Mathew, G. Lipner, X. Z. Fu, M. Antonietti, S. Blechert, X. C. Wang, *J. Am. Chem. Soc.* **2010**, *132*, 16299.
- [15] X. H. Li, J. S. Chen, X. C. Wang, J. H. Sun, M. Antonietti, *J. Am. Chem. Soc.* **2011**, *133*, 8074.
- [16] P. Ge, M. D. Scanlon, P. Peljo, X. Bian, H. Vubrel, A. O'Neill, J. N. Coleman, M. Cantoni, X. Hu, K. Kontturi, B. Liu, H. H. Girault, *Chem. Commun.* **2012**, *48*, 6484.
- [17] a) K. Herbst, G. Mogenssen, F. Huber, M. Østberg, M. S. Skjorth-Rasmussen, *Catal. Today* **2010**, *157*, 297; b) S. T. Marshall, J. W. Medlin, *Surf. Sci. Rep.* **2011**, *66*, 173.
- [18] a) B. Hinnemann, P. G. Moses, J. Bonde, K. P. Jørgensen, J. H. Nielsen, S. Hørch, I. Chorkendorff, J. K. Nørskov, *J. Am. Chem. Soc.* **2005**, *127*, 5308; b) B. Hinnemann, J. K. Nørskov, H. Topsøe, *J. Phys. Chem. B* **2005**, *109*, 2245.